Alternating Direction Projections onto Convex Sets for
Super-Resolution Image Reconstruction

Alternating Direction Projections onto Convex Sets for Super-Resolution Image Reconstruction

Bin Zhou

School of Sciences, Southwest Petroleum University, Chengdu 610050, China; e-mail: binzhou@swpu.edu.cn
Institute of Artificial Intelligence, Southwest Petroleum University, Chengdu 610500, China
Research Center of Mathematical Mechanics, Southwest Petroleum University, Chengdu 610500, China

Dong-jun Ye

School of Sciences, Southwest Petroleum University, Chengdu 610050, China; e-mail: dongjunye1996@yeah.net

Wei Wei

College of Computer Science and Engineering, Xi'an University of Technology, Xi'an 710048, China;
e-mail: weiwei@xaut.edu.cn

Marcin Woźniak

Institute of Mathematics, Silesian University of Technology, Kaszubska 23, 44-100 Gliwice, Poland;
e-mail: Marcin.Wozniak@polsl.pl

Corresponding author: binzhou@swpu.edu.cn, weiwei@xaut.edu.cn

Image reconstruction is important in computer vision and many technologies have been presented to achieve better results. In this paper, gradient information is introduced to define new convex sets. A novel POCS-based model is proposed for super resolution reconstruction. The projection on the convex sets is alternative according to the gray value field and the gradient field. Then the local noise estimation is introduced to determine the threshold adaptively. The efficiency of our proposed model is verified by several numerical experiments. Experimental results show that, the PSNR and the SSIM can be both significantly improved by the proposed model.

KEYWORDS: Reconstruction, Projection, Convex sets, Adaptive, Gradient information.

1. Introduction

In the process of image acquisition, due to limitations of imaging conditions and imaging methods, the imaging system usually cannot obtain all the information in the original scene. Therefore, how to effectively improve the image quality without modifying hardware system has always been the key problem that the imaging processing field committed to solving [17, 38, 39].

Image restoration can remove the influence of various interferences in the imaging process to some extent, and finally improve the quality of acquired images. However, it can only restore the frequency to the corresponding cutoff frequency of the diffraction limit, the energy and information outside the cutoff frequency will be lost, so it cannot really improve the resolution of the image [6]. For solve this problem, Super resolution reconstruction (SRR) is proposed.

Tsai and Huang pioneered the reconstruction of a high-resolution (HR) image from a low-resolution (LR) image sequence, and proposed a frequency-domain based restoration method [30]. Since then, SRR has become a research hotspot in the field of image processing and many methods presented based on frequency domain or space domain in the past years [15, 22, 24, 26, 30, 31].

Frequency-domain based methods transforms the image from spatial domain to frequency domain. Convolution, translation, rotation and so on the operations that are more complex in the spatial domain are simpler in the frequency domain. By transforms the SRR from space domain into the frequency domain through Fourier transform, Tsai and Huang solve SR image based on LR image sequence with global motion [30]. Rhee proposed to replace the Fourier transform with the discrete cosine transform, which improved the operation efficiency [22].

The wavelet transform as an alternative to the Fourier transform has been widely used in frequency domain-based SR algorithms. Usually it is used to decompose the input image into structurally correlated sub-images. This allows exploiting the self-similarities between local neighboring regions [2, 18]. As an example, in [2] the input image is first decomposed into subbands. Then, the input image and the high-frequency subbands are both interpolated, the results of a stationary wavelet transform of the high frequency subbands are used to improve the interpolated subbands. Finally, the super-resolved HR output is generated by combining all of these subbands using an inverse discrete wavelet transform. However, lower resolution image sequences often occur with local motion, and the frequency-domain based method is difficult to solve the spectrum of target restored image.

The methods based on Spatial-domain have strong adaptability to various motion models and prior information. Non-uniform interpolation method is the most intuitive Spatial-domain based method [31]. Projection onto convex sets (POCS) based method defines a set of constrained convex sets and ensures that their intersection contains solutions [26]. An approximate solution satisfying all the conditions of convex constraint sets can be obtained after effective iterations processed. Maximum a posterior (MAP) based method finds the high-resolution images with the highest probability of occurrence on the premise that the low-resolution image sequence is known [24].

Learning-based method is another one of the research hotspots in recent years [1, 3, 5, 10, 15, 32, 33]. Learning with PCA is an effective method. In PCA-based methods, usually the matrices representing each training image are first vectorized and then they are combined into a large matrix to obtain the covariance matrix of the training data for modeling the eigenspace. In addition, Baker and Kanade proposed an identification-based reconstruction algorithm. The reconstruction is realized by segmentation the low-resolution images and searching the matching blocks in the constructed training sample database [1]. Freeman introduces Markov network to describe the matching conditions of image blocks and sample blocks in the input low-resolution images [5]. On this basis, Wang extended the Markov network model and proposed a blind restoration method to estimate the point spread function (PSF) parameters of pixel sensors [32]. In recent years, learning-based research has been inclined to convolutional neural network (CNN). Dong introduced CNN to directly learn the mapping between LR image and HR image, then realized the super-resolution reconstruction based on a single image [3]. Deeply-recursive convolutional network (DRCN) is proposed to learn mapping, then

the difficulty of training can be reduced by the application of recursive monitoring and jump connection [10]. Lai and Huang proposed LapSRN (Laplacian Pyramid Super-Resolution Network) to gradually reconstruct the sub-band residuals of high-resolution images [12].

POCS-based methods are more advantageous to use prior knowledge and they are still efficient to some complex cases with motions or different observation models. These methods were first proposed by Stark and Oskoui [26]. Tekalp proposes an improved pocs-based method, which considers the effecting of sensor blurring and observation noise, and shows that the POCS formulation presented for the high-resolution image reconstruction problem can also be used as a new method for the restoration of spatially invariant blurred images [28]. On this basis, Patti and his partner came up with a new formula that takes into consideration blurring due to sensor-based motion, integration and noise [19].

However, in traditional methods based on POCS, calculation is often expensive, the solution is not unique and often affected by serious artifacts.

Tom and Katsaggelos proposed to define constraint sets by ellipsoids (instead of regular spheres) and determined the unique target solution [29]. Yu made improvements to the Point Spread Function (PSF). The blur PSF centered at an edge pixel is weighted by an exponential function, so the PSF coefficients decrease along the orthogonal direction of the edge and reduce the quantity of Gibbs artifacts present [37]. Based on the visual mechanism, Liu proposed the variability threshold to deal with the super-resolution reconstruction of infrared images, improved contrast of results [14]. After introducing fractional calculus to convex set projection, Lei proposed a super-resolution enhancement algorithm for UAV images. The high-resolution and low-resolution reference frames can be enhanced by fractional calculus operator, and the PSF of POCS is simulated by a fractional integral filter instead of Gaussian filter [13].

In this paper, gradient information is introduced to build novel convex sets and the artifacts can be suppressed more efficiently in the reconstruction. Local adaptive constraint thresholds and a dynamic relax factor are used to improve the calculation efficiency. Then alternating direction projections on the novel convex sets are presented to solve the super-resolution reconstruction problem. Finally, some numerical experiments are carried out to verify the accuracy and efficiency of proposed algorithm.

The rest of this paper is arranged as follows. The fundamentals of POCS method are delineated in Section 2. In Section 3, novel convex sets and an alternative projections algorithm are proposed. Experiments and results are demonstrated in Section 4 after some real low-resolution image sequences are prepared [4, 8, 9, 20, 21, 25, 34, 35, 37].

2. Fundamentals

2.1. Super-resolution Reconstruction

There are many ways to improve spatial resolution through hardware, such as increase the pixel density or chip size. However, the high cost for high precision optics and image sensors is a negative factor in commercial promotion.

Super-resolution reconstruction can help to improve the resolution of images without modifying hardware system so as to reduce funds. Therefore, SRR has been developed in image processing fields [17]. Figure 1 shows the degradation procedure and the meaning of super resolution reconstruction.

Based on the aliasing relationship between SR image and LR image sequence with global motion in frequency domain, Tsai and Huang takes the Fourier transform of the LR image sequence, solve the spectrum of the SR image, and the SR image is obtained by the inverse Fourier transform to spectrum [30].

The non-uniform interpolation is the simplest method of super-resolution reconstruction. SRR is regarded as an Image interpolation problem, where the restoration result can be obtained through different interpolation methods [7].

POCS-based methods are a kind of the iteration method of SRR. In the classical POCS method, various constraints on the target HR image are defined as closed convex sets in the HR image space, target solutions are in their intersection [24].

MAP-based methods are based on probability. They regard super-resolution (SR) image as the solution of a complex optimization problem. Under the premise

Figure 1

Image degradation procedure and supper resolution reconstruction
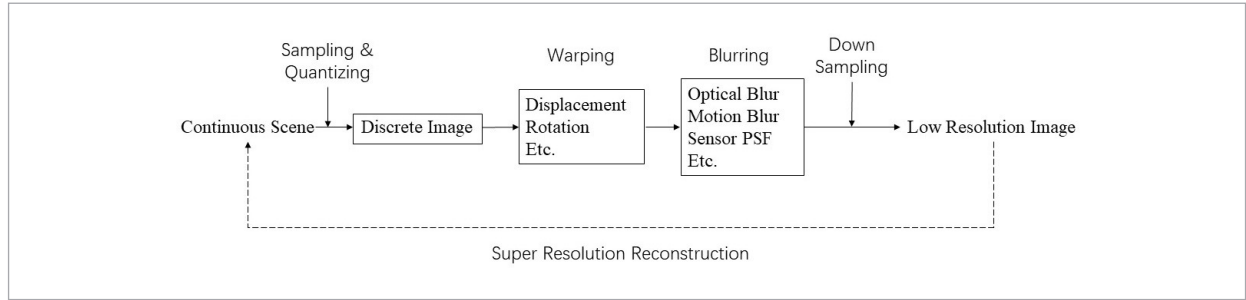
of knowing LR image sequence, HR image with the maximum posterior probability is taken as the solution [1].

POCS-based methods can effectively find feasible solutions to complex optimization problems, and their advantages lie in their simple ideas, flexible method forms and convenient addition of prior knowledge.

2.2. Projections on Convex Sets

In traditional POCS-based methods, the unknown signal u is assumed to be an element of an appropriate Hilbert space H [36]. Each prior information or constraint restricts the solution to a closed convex set in H. Thus, for m pieces of information, there are m corresponding closed convex sets $C_i \in H$, and $i = 1, 2, \cdots, m$, $u \in C_0 = \bigcap_{i=1}^{m} C_i$, provided that the intersection C_0 is nonempty. Given the constraint sets C_i and their respective projection operators P_i, the sequence generated by

$$f_{k+1} = T_m T_{m-1} \cdots T_1 f_k, k = 0, 1, \cdots \tag{1}$$

where the relaxed projection operator $T_i = (1 - \lambda_k) I + \lambda_k P_i, 0 < \lambda_k < 2$, and f_0 means an initial estimation of u. It can be get that f_k converges weakly to a feasible solution in the intersection C_0 of the consistent with the prior constraints, and therefore, a feasible solution satisfied the constraints can be approximated by efficient iteration.

2.2.1. Image as a Linear System

The image function can be represented as a linear combination of Dirac pulses at each point (a,b) covering the entire image plane.

$$f(x,y) = \iint_{R^2} f(a,b)\delta(a-x, b-y)\, da\, db. \tag{2}$$

The response g of LSV (linear shift-varying) system L to input image f can be expressed as

$$
\begin{aligned}
g(x,y) &= L\{f(x,y)\} \\
&= \iint_{R^2} f(a,b) L\{\delta(a-x, b-y)\}\, da\, db \\
&= \iint_{R^2} f(a,b) h(a,b; x,y)\, da\, db,
\end{aligned}
\tag{3}
$$

where h is the shift-varying impulse response of L.

2.2.2. POCS-based Reconstruction

When f is a $M_1 \times M_2$ high-resolution image, and $S(n_1, n_2)$ denotes the HR image support area of LR pixel point (n_1, n_2), including the observation noise v, one pixel value $g(n_1, n_2)$ of low-resolution image can be expressed as [16]

$$
\begin{aligned}
g(n_1, n_2) &= L\{f(m_1, m_2)\} + v(n_1, n_2) \\
&= \sum_{(m_1, m_2) \in S} f(m_1, m_2) h(n_1, n_2; m_1, m_2) + v(n_1, n_2).
\end{aligned}
\tag{4}
$$

Assume that the statistical characteristics of the noise process are known, then introduce following closed, convex constrain sets (one for each observed blurred image pixel)

$$
\begin{aligned}
C_{n_1, n_2} = \{ &f(m_1, m_2) : |r_f(n_1, n_2)| \le \delta_0 \\
&\wedge (m_1, m_2) \in S \},
\end{aligned}
\tag{5}
$$

where δ_0 is an a prior bound reflecting the statisti-

cal confidence and the actual image is a member of the set C_{n_1,n_2}. r_f denotes the residual between the real imaging system and the discrete linear shift-varying system, more in detailed as

$$r_f\left(n_1,n_2\right)=g\left(n_1,n_2\right)$$
$$-\sum_{\left(m_1,m_2\right)\in S} f\left(m_1,m_2\right)h\left(n_1,n_2;m_1,m_2\right). \tag{6}$$

When estimated image f approximates to the actual image, r_f approximates to the noise v.

The projection of an arbitrary $f\left(m_1,m_2\right)$, onto C_{n_1,n_2} can be defined as

$$P_{n_1,n_2}=\begin{cases}f\left(m_1,m_2\right)+\dfrac{\left(r_f-\delta_0\right)h\left(n_1,n_2;m_1,m_2\right)}{\sum_{\left(w_1,w_2\right)\in S}h^2\left(n_1,n_2;w_1,w_2\right)},r_f>\delta_0,\\[4pt] f\left(m_1,m_2\right), \qquad\qquad\qquad\qquad \left|r_f\right|<\delta_0,\\[4pt] f\left(m_1,m_2\right)+\dfrac{\left(r_f+\delta_0\right)h\left(n_1,n_2;m_1,m_2\right)}{\sum_{\left(w_1,w_2\right)\in S}h^2\left(n_1,n_2;w_1,w_2\right)},r_f<-\delta_0\end{cases} \tag{7}$$

It is easy to design an efficient algorithm solving above POCS-based super-resolution reconstruction model. However, artifacts can still be found on the edges of the reconstructed image because the steep and fast changes are treated as the plain region. The constraint threshold is set fixed and the difference of the image locals are ignored, so it can be found that important image details are lost or there is insufficient denoising. Aiming at these problems, an improved POCS-based model is proposed in the next section.

3. Fast Projections on Novel Convex Sets

3.1. Gradient-based Convex Sets

Traditional projections on convex sets (POCS) methods build the model only according to the observed image and the pixel degradation from a high resolution image to a low-resolution one. More exactly, as the estimated image f close nearly to the actual image u, r_f will also approximate the distribution and their statistical characteristics are almost the same. Based on this, convex constraint sets can be defined in the probability sense with the solution included, and iterative projec-

tion can be introduced to get an approximated solution. The POCS model associates a pixel in the LR image with an area in the HR image. It overlaps spatially the outputs of two adjacent pixels in the LR image and the conflicts in the overlapping areas should be properly treated during the projection. However, it is easy

Figure 2
An overlapping region
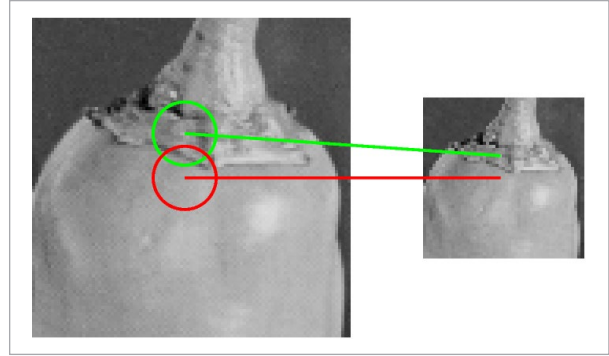
to cause considerable estimation error and artifacts, especially if the two pixels vary greatly, for example, they are near the edges.

In order to reduce the artifacts and improve the result, this paper proposes a novel reconstruction model with better suppression to the error fluctuation of the estimation on neighbor pixels. Firstly, gradient-based compound convex sets are introduced as follows.

For continuous function $u\left(x,y\right)$, the gradient is denoted as

$$\nabla u\left(x,y\right)=\left[\frac{\partial u}{\partial x}\left(x,y\right),\frac{\partial u}{\partial y}\left(x,y\right)\right]^T. \tag{8}$$

As f, g are discrete digital images, the gradient can be denoted by finite difference scheme as follows

$$\nabla f\left(m_1,m_2\right)\approx\begin{bmatrix}f\left(m_1+1,m_2\right)-f\left(m_1,m_2\right)\\ f\left(m_1,m_2+1\right)-f\left(m_1,m_2\right)\end{bmatrix}$$
$$\nabla g\left(n_1,n_2\right)\approx\begin{bmatrix}g\left(n_1+1,n_2\right)-g\left(n_1,n_2\right)\\ g\left(n_1,n_2+1\right)-g\left(n_1,n_2\right)\end{bmatrix}. \tag{9}$$

A gradient-based compound convex set can be defined as

$$C^G_{n_1,n_2} = \{ f(m_1,m_2) : |r_f(n_1,n_2)| \le \delta_0$$
$$\wedge |r_f^G(n_1,n_2)| \le \delta^G \wedge (m_1,m_2) \in S \}. \tag{10}$$

Here

$$r_f^G(n_1,n_2) = \nabla g(n_1,n_2)$$
$$- \sum_{(m_1,m_2)\in S} \nabla f(m_1,m_2) h(n_1,n_2;m_1,m_2).$$

and δ^G means the gradient threshold.

3.2. Alternating Direction Projection

After above gradient-based convex sets are defined, the new projection operator corresponding to the convex set can be denoted as follows.
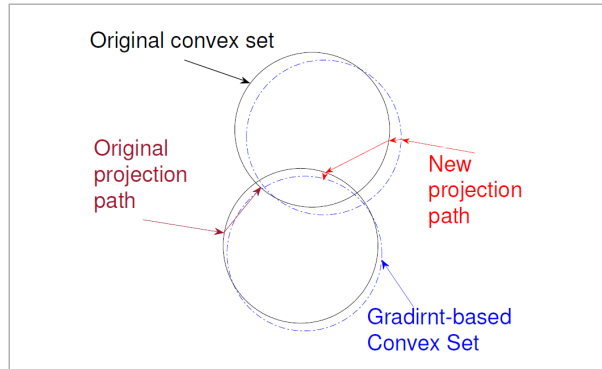
$$P_{n_1,n_2} = f(m_1,m_2) + df(m_1,m_2) + df_G(m_1,m_2), \tag{11}$$

$$df = \begin{cases} \dfrac{[r_f - \delta_0] h(n_1,n_2;m_1,m_2)}{\sum_{(w_1,w_2)\in S} h^2(n_1,n_2;w_1,w_2)}, & r_f > \delta_0, \\ 0, & |r_f| \le \delta_0, \\ \dfrac{[r_f + \delta_0] h(n_1,n_2;m_1,m_2)}{\sum_{(w_1,w_2)\in S} h^2(n_1,n_2;w_1,w_2)}, & r_f < -\delta_0, \end{cases}$$

$$df_G = \begin{cases} \dfrac{[r_f^G - \delta^G] h(n_1,n_2;m_1,m_2)}{\sum_{(w_1,w_2)\in S} h^2(n_1,n_2;w_1,w_2)}, & r_f^G > \delta^G, \\ 0, & |r_f^G| \le \delta^G, \\ \dfrac{[r_f^G + \delta^G] h(n_1,n_2;m_1,m_2)}{\sum_{(w_1,w_2)\in S} h^2(n_1,n_2;w_1,w_2)}, & r_f^G < -\delta^G. \end{cases} \tag{12}$$

Figure 3
Alternating Direction Projection

Assume μ_i is a real pixel value, and z_i means the estimation. Here we will illustrate that $\Pr(-k < z_i - \mu_i < k)$ is bigger in C_{new} than C.

Both traditional POCS methods and improved POCS method limit the value of $r_i = z_i - \mu_i$.

As shown in Figure 4, the red area represents the truncated part, with a cumulative probability of 0. The blue area is the change in probability for the rest part. It can be seen that their distribution is more concentrated. In other words, gradient-based compound convex sets can reduce the noise fluctuation, thus reducing the probability of gray scale jump change.

Figure 4
The truncated probability density
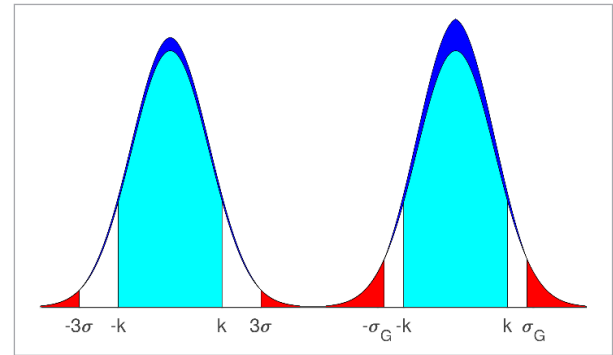

3.3. Local Adaptive Thresholds

When estimated image f approximates to the actual image, $r^{(f)}$ are identical to the residual between observation and the simulation observation. Hence, the bound δ_0 is determined from the statistics of the noise process so that the actual image is a member of the set with in a certain statistical confidence.

In traditional POCS algorithms, δ_0 is constant, ignoring the distinction between the global noise and the local noise, using the same δ_0 to each pixel points.

In general, a larger δ_0 means that fewer points need to be corrected, causing some points that should be corrected to be ignored. On the contrary, smaller δ_0 means that more pixel points need to be corrected, which will often lead to destroying feature points.

The threshold δ_0 should be replaced by an adaptive version. Due to the local smoothness of natural images, the gray values of pixels belonging to the same structure are usually at the same level [11, 27]. Therefore, the standard deviation of these gray values can be approximated as the standard deviation of noise.

Figure 5

Effects of fixed threshold
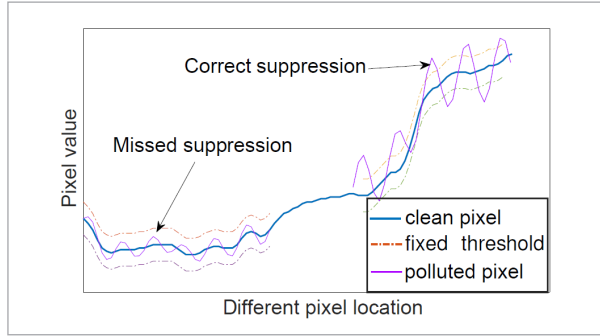
A proper neighborhood can be determined by local total variation statistics. The radius d can be optimized by

$$\max_{d} \quad \frac{\partial}{\partial d} MTV(g,d)$$

$$s.t.$$

$$\begin{cases} MTV(f,d) = \dfrac{1}{|\Omega_d|} \displaystyle\sum_{(i,j)\in\Omega_d} |\nabla g(i,j)|, \\ d \in [d_1, d_2]. \end{cases} \tag{13}$$

where $\Omega_d = U(m_1, m_2; d)$ denotes the neighborhood of point (m_1, m_2) with radius d. MTV denotes the mean of local total variation statistics. If the local homogeneous region is approximated by Ω_d, then the standard deviation σ can be used to a confidential set $\delta_0 = 3\sigma$.

3.4. Dynamic Relax Factor

At the beginning of traditional POCS, the convergence speed is fast, and as the iterations go, the convergence speed is slower and slower. A relax factor can be used to accelerate the iteration and maintain accuracy.

When λ_i approaches 0, T_i is approximately equal to I, the projection essentially stagnant. When λ_i is set to be greater than 1, the projection will be accelerated. $\lambda_i = 1$ means unrelaxed projection.

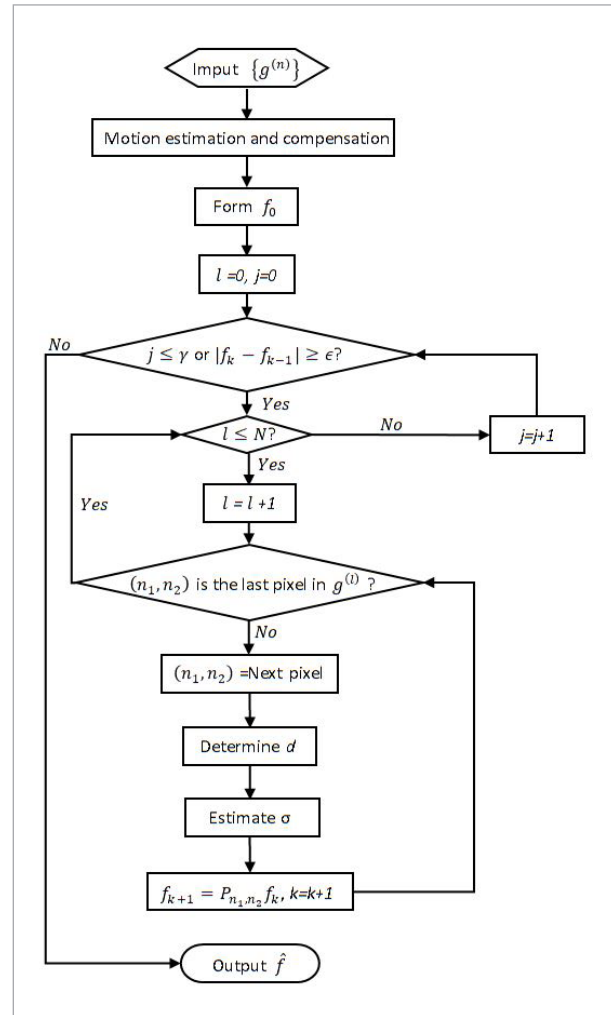According to our requirements, a dynamic relax factor can be used

$$\lambda_i = 1 + e^{-i}. \tag{14}$$

It accelerates at the beginning of the iteration, slows down in the middle, and adapts to the high requirements for precision in the later stage.

4. The Proposed Algorithm and Numerical Experiments

4.1. Algorithm

Figure 6

Full flow charts

Based on Section 3, an alternating direction projections algorithm can be presented as follows.

Step 1. Compute the initial estimation f_0 by interpolating on the LR image.

Step 2. Perform motion estimation and compensation on the LR image sequence $\{g^{(n)}\}$.

Step 3. Determine the adaptive thresholds by local noise estimation.

Step 4. Compute the gradient-based convex sets and alternative projection on them until stop condition satisfied.

The full flow charts for the proposed algorithm is shown in Figure 6. For convenience of representation, symbols that do not appear in the text are used. $\{g^{(n)}\}$ is the LR image sequence, γ is the upper limit of the number of cycles, $\mathring{a}$ is a parameter and N is the number of pixels in g^l.
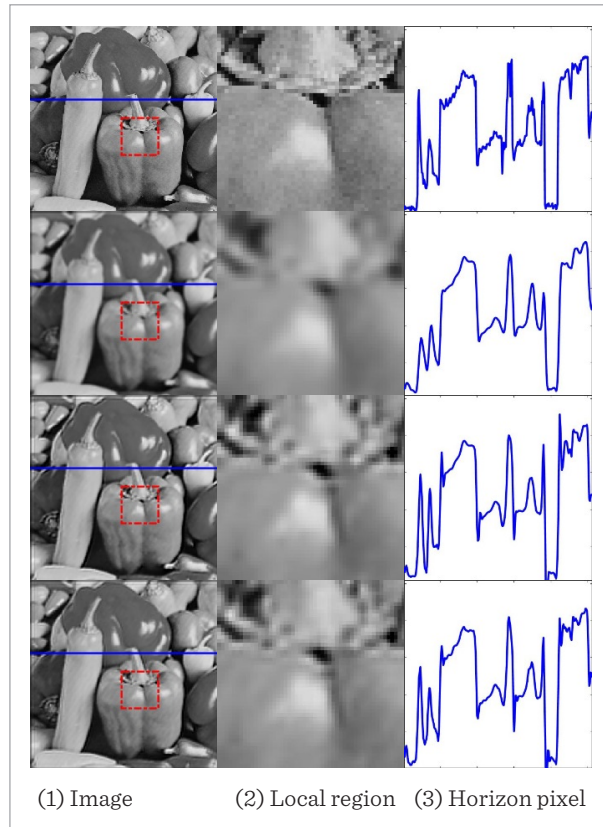
4.2. Experiments

To verify the performance of the proposed method, real image as a reference is necessary, but in practice it is unknown. To simulate the imaging process in reality to some extent, an image of size 256×256 is affected by a linear shift-varying system and down-sampling with an interval of 1, generate a LR image.

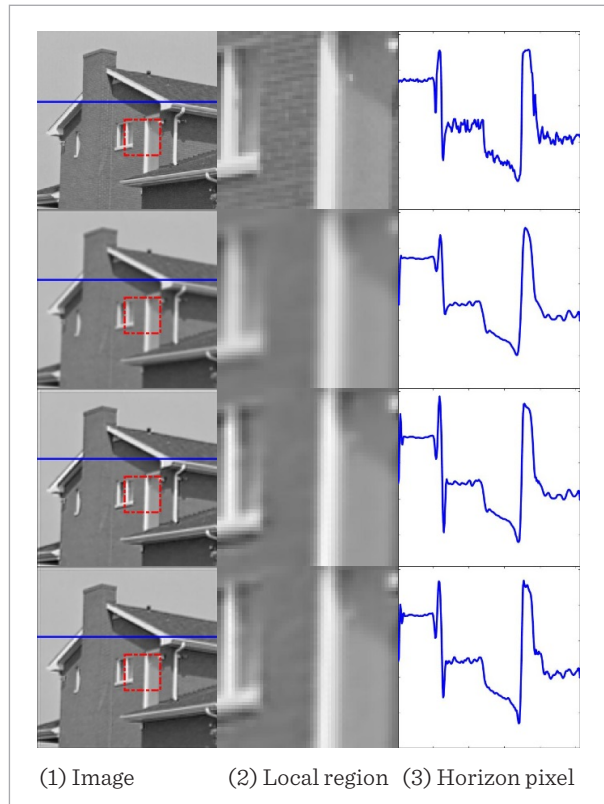Figure 7 shows the reconstruction results computed from the LR peppers image. The first row is the origi-nal image and the second row means an initial inter-polation of the LR image. The third row and the last one show the traditional POCS reconstruction result and our result. The details of the image are restored to a certain extent, which is clearer than the initial in-terpolation, but there are some artifacts at the edges of the image, and smaller details are lost. Compared with it, the detail of our result is improved, and the ar-tifact of the edge is reduced. A comparison of pixels on the blue line is also shown in the figure.

Figure 8

House image reconstruction

(1) Image   (2) Local region   (3) Horizon pixel

Figure 7

Peppers image reconstruction

(1) Image   (2) Local region   (3) Horizon pixel

The experimental results show that the proposed method is better than the traditional method in the aspect of visual effect. Two similar experimental re-sults with other image are given in Figures 8 and 9. In addition, in order to observe the performance of the algorithm under some special circumstances, we chose a remote sensing image RSimg for the experi-ment. Figure 10 gives the reconstruction results.
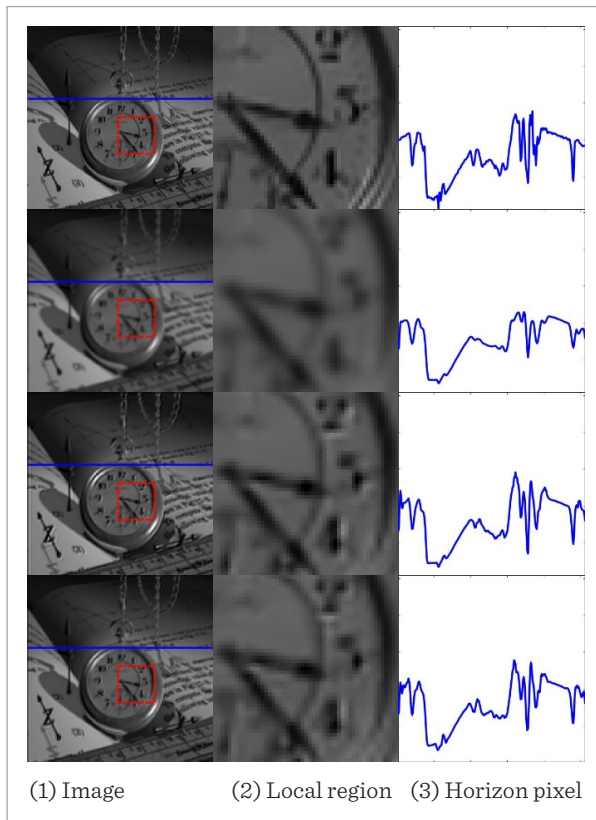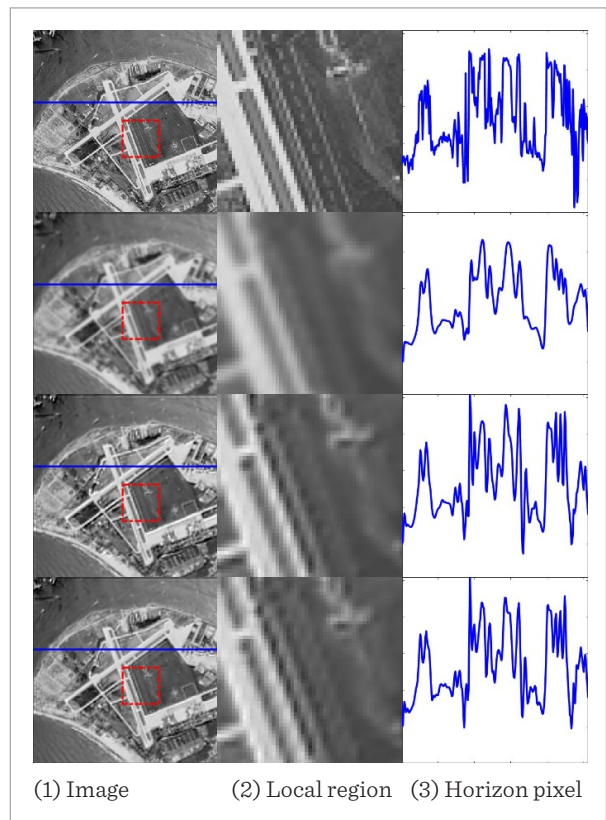
Figure 9

Clock image reconstruction

(1) Image   (2) Local region   (3) Horizon pixel

Figure 10

Remote Sensing image reconstruction

(1) Image   (2) Local region   (3) Horizon pixel

To achieve convincing evaluation of reconstruction results, we calculated the structure similarity (SSIM) and peak signal to noise ratio (PSNR) of different results as shown in Table 1.

Table 1

Evaluation of four images reconstruction

| Evaluation	Image	Interpolation	POCS	Proposed
PSNR	Peppers	23.54	26.61	28.26
	House	26.28	29.07	31.02
	Clock	26.39	28.98	31.03
	RSimg	20.02	21.41	22.42
SSIM	Peppers	0.5187	0.6067	0.6717
	House	0.3412	0.4022	0.4730
	Clock	0.5563	0.6741	0.7344
	RSimg	0.3375	0.4820	0.5279

Table 2

Peppers image reconstruction with different noise level

Noise level	Interpolation	POCS	Proposed
20db	23.40	26.02	27.45
25db	23.50	26.42	27.98
30db	23.52	26.55	28.18
35db	23.53	26.59	28.23
40db	23.54	26.61	28.26

To verify the robust of proposed method, we apply the proposed method to peppers image with different Gaussian noise. The PSNR results are shown in Table 2.

As an additional extension, we apply the proposed method to a color peppers image. Through the super-resolution reconstruction of each channel of the color image, we can get a reconstruction result as shown in Figure 11. The first row is the original image and the second is

Figure 11

Color peppers image reconstruction

(1) Image   (2) Local region   (3) Horizon pixel
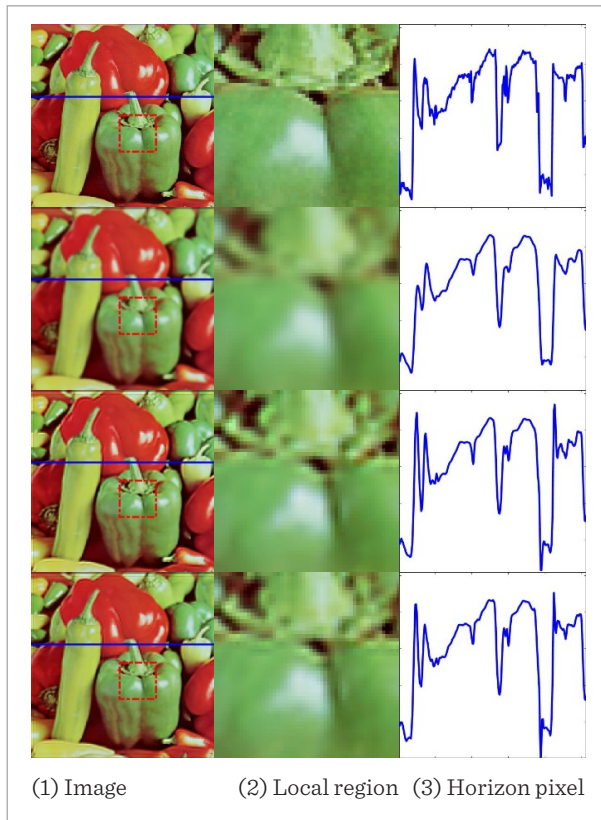
the interpolation of LR image, traditional POCS result and our result are shown in last two rows.

The experimental results show some advantages of the proposed method in some color images reconstruction cases. Gradient-based convex sets and local adaptive constraint thresholds are helpful to relief

the over-smoothing in reconstruction images, well reconstruct the image details (such as textures) and suppress the artifact near the edge to some extent. As shown in Table 3, some evaluations such as PSNR and SSIM can be significantly improved by proposed method than the traditional POCS method.

Table 3

Evaluation of the color peppers image reconstruction

Evaluation	Interpolation	POCS	Proposed
PSNR	25.10	29.04	30.81
SSIM	0.5658	0.6543	0.7132

5. Conclusion

This paper proposes an improved POCS-based super resolution reconstruction method. In this method, gradient-based convex sets and alternating direction projection are applied in the iterative reconstruction. Local adaptive constraint thresholds can improve the accuracy of the method. Experimental results and two evaluations (PSNR and SSIM) show that the improved method can achieve better reconstruction result, well suppress the artifacts and relief the over-smoothing in some cases. In the future work, we will continue to work on the mechanism of artifact formation, and more efficient reconstruction based on feature information.

Acknowledgement

References

1. Baker, S., Kanade, T. Hallucinating Faces. Proceedings Fourth IEEE International Conference on Automatic Face and Gesture Recognition, 2000, 83-88.

2. Demirel, H., Anbarjafari, G. Image Resolution Enhancement by Using Discrete and Stationary Wavelet Decomposition. IEEE Transactions on Image Processing, 2010, 20(5), 1458-1460. https://doi.org/10.1109/TIP.2010.2087767

3. Dong, C., Loy, C. C., He, K., Tang, X. Image Super-Resolution Using Deep Convolutional Networks. IEEE Transactions on Pattern Analysis and Machine Intelligence, 2015, 38(2), 295-307. https://doi.org/10.1109/TPAMI.2015.2439281

4. Fan, X., Song, H., Fan, X., Yang, J. Imperfect Information Dynamic Stackelberg Game Based Resource Allocation Using Hidden Markov for Cloud Computing. IEEE

Transactions on Services Computing, 2016, 11(1), 78-89. https://doi.org/10.1109/TSC.2016.2528246

5. Freeman, W. T., Jones, T. R., Pasztor, E. C. Example-based Super-resolution. IEEE Computer Graphics and Applications, 2002, (2), 56-65. https://doi.org/10.1109/38.988747

6. Hunt, B. R. Super-Resolution of Imagery: Understanding the Basis for Recovery of Spatial Frequencies Beyond the Diffraction Limit. In 1999 Information, Decision and Control. Data and Information Fusion Symposium, Signal Processing and Communications Symposium and Decision and Control Symposium. Proceedings (Cat. No. 99EX251), 1999, 243-248. https://doi.org/10.1109/IDC.1999.754163

7. Irani, M., Peleg, S. Improving Resolution by Image Registration. CVGIP: Graphical Models and Image Processing, 1991, 53(3), 231-239. https://doi.org/10.1016/1049-9652(91)90045-L

8. Ke, Q., Zhang, J., Song, H., Wan, Y. Big Data Analytics Enabled by Feature Extraction Based on Partial Independence. Neurocomputing, 2018, 288, 3-10. https://doi.org/10.1016/j.neucom.2017.07.072

9. Ke, Q., Zhang, J., Wei, W., Połap, D., Woźniak, M., Kośmider, L., Damaševĭcius, R. A Neuro-Heuristic Approach for Recognition of Lung Diseases from X-Ray Images. Expert Systems with Applications, 2019, 126, 218-232. https://doi.org/10.1016/j.eswa.2019.01.060

10. Kim, J., Kwon Lee, J., Mu Lee, K. Deeply-Recursive Convolutional Network for Image Super-Resolution. In Proceedings of the IEEE Conference on Computer Vision and Pattern Recognition, 2016, 1637-1645. https://doi.org/10.1109/CVPR.2016.181

11. Kim, K. I., Kwon, Y. Single-Image Super-Resolution Using Sparse Regression and Natural Image Prior. IEEE Transactions on Pattern Analysis and Machine Intelligence, 2010, 32(6), 1127-1133. https://doi.org/10.1109/TPAMI.2010.25

12. Lai, W. S., Huang, J. B., Ahuja, N., Yang, M. H. Deep Laplacian Pyramid Networks for Fast and Accurate Super-Resolution. In Proceedings of the IEEE Conference on Computer Vision and Pattern Recognition, 2017, 624-632. https://doi.org/10.1109/CVPR.2017.618

13. Lei, J., Zhang, S., Luo, L., Xiao, J., Wang, H. Super-Resolution Enhancement of UAV Images Based on Fractional Calculus and POCS. Geo-spatial Information Science, 2018, 21(1), 56-66. https://doi.org/10.1080/10095020.2018.1424409

14. Liu, J., Dai, S., Guo, Z., Zhang, D. An Improved POCS Super-Resolution Infrared Image Reconstruction Al-gorithm Based on Visual Mechanism. Infrared Physics & Technology, 2016, 78, 92-98. https://doi.org/10.1016/j.infrared.2016.07.010

15. Nasrollahi, K., Moeslund, T. B. Super-Resolution: A Comprehensive Survey. Machine Vision and Applications, 2014, 25(6), 1423-1468. https://doi.org/10.1007/s00138-014-0623-4

16. Ozkan, M. K., Tekalp, A. M., Sezan, M. I. POCS-Based Restoration of Space-Varying Blurred Images. IEEE Transactions on Image Processing, 1994, 3(4), 450-454. https://doi.org/10.1109/83.298398

17. Park, S. C., Park, M. K., Kang, M. G. Super-Resolution Image Reconstruction: A Technical Overview. IEEE signal processing magazine, 2003, 20(3), 21-36. https://doi.org/10.1109/MSP.2003.1203207

18. Patil, V. H., Bormane, D. S., Pawar, V. S. Super Resolution Using Neural Network. In 2008 Second Asia International Conference on Modelling & Simulation (AMS). IEEE, 2008, 492-496. https://doi.org/10.1109/AMS.2008.140

19. Patti, A. J., Sezan, M. I., Tekalp, A. M. High-Resolution Image Reconstruction from a Low-Resolution Image Sequence in the Presence of Time-Varying Motion blur. In Proceedings of 1st International Conference on Image Processing, 1994, 1, 343-347.

20. Qi, Y. Information Potential Fields Navigation in Wireless Ad-Hoc Sensor Networks. Sensors, 11(5), 4794-4807. https://doi.org/10.3390/s110504794

21. Qiang, Y., Zhang, J. A Bijection Between Lattice-Valued Filters and Lattice-Valued Congruences in Residuated Lattices. Mathematical Problems in Engineering, 2013, Article ID 908623. https://doi.org/10.1155/2013/908623

22. Rhee, S., Kang, M. G. Discrete Cosine Transform Based Regularized High-Resolution Image Reconstruction Algorithm. Optical Engineering, 1999, 38(8), 1348-1356. https://doi.org/10.1117/1.602177

23. Sanguansat, P. Face Hallucination Using Bilateral-Projection-Based Two-Dimensional Principal Component Analysis. In 2008 International Conference on Computer and Electrical Engineering. IEEE, 2008, 876-880. https://doi.org/10.1109/ICCEE.2008.99

24. Schultz, R. R., Stevenson, R. L. Extraction of High-Resolution Frames from Video Sequences. IEEE Transactions on Image Processing, 1996, 5(6), 996-1011. https://doi.org/10.1109/83.503915

25. Song, H., Li, W., Shen, P., Vasilakos, A. Gradient-Driven Parking Navigation Using a Continuous Information Potential Field Based on Wireless Sensor Network.

Information Sciences, 2017, 408, 100-114. https://doi.org/10.1016/j.ins.2017.04.042

26. Stark, H., Oskoui, P. High-Resolution Image Recovery from Image-Plane Arrays, Using Convex Projections. JOSA A, 6(11), 1989, 1715-1726. https://doi.org/10.1364/JOSAA.6.001715

27. Tappen, M. F., Russell, B. C., Freeman, W. T. Exploiting the Sparse Derivative Prior for Super-Resolution and Image Demosaicing. In In IEEE Workshop on Statistical and Computational Theories of Vision. 2003.

28. Tekalp, A. M., Ozkan, M. K., Sezan, M. I. High-Resolution Image Reconstruction from Lower-Resolution Image Sequences and Space-Varying Image Restoration. In [Proceedings] ICASSP-92, 1992 IEEE International Conference on Acoustics, Speech, and Signal Processing. 1992, 3, 169-172. https://doi.org/10.1109/ICASSP.1992.226249

29. Tom, B. C., Katsaggelos, A. K. Iterative Algorithm for Improving the Resolution of Video Sequences. In Visual Communications and Image Processing'96. International Society for Optics and Photonics. 1996, 2727, 1430-1438. https://doi.org/10.1117/12.233218

30. Tsai, R.Y., Huang, T.S. Multiframe Image Restoration and Registration. Advance Computer Visual and Image Processing, 1984, 1, 317-339.

31. Ur, H., Gross, D. Improved Resolution from Subpixel Shifted Pictures. CVGIP: Graphical Models and Image Processing, 1992, 54(2), 181-186. https://doi.org/10.1016/1049-9652(92)90065-6

32. Wang, Q., Tang, X., Shum, H. Patch Based Blind Image Super Resolution. In Tenth IEEE International Conference on Computer Vision (ICCV'05). 2005, 1, 709-716.

33. Wang, Z., Yi, P., Jiang, K., Jiang, J., Han, Z., Lu, T., Ma, J. Multi-Memory Convolutional Neural Network for Video Super-Resolution. IEEE Transactions on Image Processing, 2018, 28(5), 2530-2544. https://doi.org/10.1109/TIP.2018.2887017

34. Xu, Q., Wang, L., Hei, X. H., Shen, P., Shi, W., Shan, L. GI/Geom/1 Queue Based on Communication Model for Mesh Networks. International Journal of Communication Systems, 2014, 27(11), 3013-3029.

35. Yang, X. L., Zhou, B., Feng, J., Shen, P. Y. Combined Energy Minimization for Image Reconstruction from Few Views. Mathematical Problems in Engineering, 2012, Article ID 154630. https://doi.org/10.1155/2012/154630

36. Youla, D. C., Webb, H. Image Restoration by the Method of Convex Projections: Part 1 Theory. IEEE Transactions on Medical Imaging, 1982, 1(2), 81-94. https://doi.org/10.1109/TMI.1982.4307555

37. Yu, J., Xiao, C., & Su, K. A Method of Gibbs Artifact Reduction for POCS Super-Resolution Image Reconstruction. In 2006 8th International Conference on Signal Processing. 2006, 2. https://doi.org/10.1109/ICOSP.2006.345717

38. Zhou, B., Duan, X., Wei, W., Ye, D., Wozniak M. and Damasevicius, R. An Adaptive Local Descriptor Embedding Zernike Moments for Image Matching. IEEE Access, 2019, 7, 183971-183984. https://doi.org/10.1109/ACCESS.2019.2960203

39. Zhou, B., Duan, X., Ye, D., Wei, W., Wozniak, M. and Damasevicius, R. Heterogeneous Image Matching via a Novel Feature Describing Model. Applied Sciences, 2019, 9(22), 4792. https://doi.org/10.3390/app9224792